8th International IFAC Symposium on
Dynamics and Control of Process Systems
Preprints Vol.2, June 6-8, 2007, Cancún, Mexico

OPTIMAL STRATEGIES FOR CONTROLLING PARTICLE SIZE IN ANTISOLVENT CRYSTALLIZATION OPERATIONS

S. M. Nowee[1], A. Abbas[2], J.A. Romagnoli[3*] and P. Yeo[4]

[1] *School of Chemical and Biomolecular Engineering, University of Sydney, Australia*
[2] *Division of Engineering Science and Technology, University of New South Wales Asia, Singapore*
[3] *Department of Chemical Engineering, Louisiana State University, USA*
[4] *School of Chemical and Biomedical Engineering, Nanyang Technological University, Singapore*

Abstract: In this paper, a model-based optimal strategy is presented for the control of particle size in antisolvent crystallization. Size is controlled on demand by dynamic optimization using a population balance based model. Knowledge of the ternary solute-solvent-antisolvent equilibrium and crystallization kinetics is crucial in this strategy and are both experimentally identified and incorporated in the model. The optimization is capable of determining the optimal antisolvent feed profile that achieves a desired particle size. Experimental validation of the strategy is carried out and presented herein. Such a strategy stands as a key solution to antisolvent operations ubiquitous in the pharmaceutical and fine chemicals industries.

Keywords: antisolvent crystallization, optimization, particle size, crystal size distribution, nucleation, growth, parameter estimation, FBRM, feed profile, pharmaceutical.

1. INTRODUCTION

Crystallization is a widely used technique in solid-liquid separation processes. The driving force in crystal formation is supersaturation. The trend of supersaturation generation during the process has a direct and significant role on crystal characteristics such as size, morphology and purity. There is a number of ways one can affect supersaturation including cooling and evaporation. In the last decade, salting-out as a means to induce supersaturation has been drawing more attention. In this method a secondary solvent known as antisolvent or precipitant is added to the solution resulting in the reduction of the solubility of the solute in the original solvent and consequently supersaturation is generated. Antisolvent crystallization is an advantageous method where the substance to be crystallized (solute) is highly soluble, has solubility that is a weak function of temperature, is heat sensitive, or unstable in high temperatures. This technique is an energy-saving alternative to evaporative crystallization, if the antisolvent can be separated at low (energy) costs.

The rate of supersaturation generation is highly dependent on antisolvent addition rate. In operations where there is poor mixing regimes high local supersaturation at antisolvent induction point exists leading to excess primary nucleation and consequently resulting in fine crystal particle formation that easily tend to agglomerate (Takiyama et al. 1998). This fact and the strive for better operational policies have been the interest of many recent investigations.

Experimental works looking at the effect of various operating conditions are numerous. Takiyama et al. (1998) investigated the effect of different concentrations of aqueous and antisolvent solutions on crystal shape and distribution. The main variable they studied was supersaturation. They proposed a mechanistic formulation in finding the relation between nucleation and supersaturation. Other works considered antisolvent concentration and feed rate effects on final crystal habit (Holmback & Rasmusan (1999), Oosterhof et al. (1999a), Taboada et al. (2000), Kaneko et al. (2002), Doki et al. (2002),

Kitamura & Sugimoto (2003) and Yu et al. (2005)). Since these kinds of systems are complex due to three components interacting with each other in two phases some thermodynamic and mass transfer studies are essential. Ho-Gutierrez et al. (1994) plotted solubility and phase diagrams for the two ternary systems of polyethylene glycol and aqueous solutions of sodium sulphate and sodium chloride. Oosterhof et al. (1999b) also investigated different antisolvents for sodium carbonate-water system and they found a correlation between salt solubility and water-antisolvent mixture decomposition at constant temperature.

Unlike most works that study inorganic solute crystallization by organic antisolvents, Holmback & Rasmusan (1999) and Yu et al. (2005) considered organic solutions and water as second solvent. Size and morphology of benzoic acid crystals from ethanol-water system were investigated by Holmback & Rasmusan's (1999) who varied the feed and bulk solution composition and feed rate. They observed that supersaturation mainly governs the mean size while solvent composition has significant effect on the crystal shape. Agglomeration and habit of paracetamol crystals were the focus of the study by Yu et al. (2005) who varied the agitation speed and feed rate. In their study they concluded that low agitation speed and high feed rate will result in excessive nucleation due to high local supersaturation leading to highly agglomerated product with lower mean size.

In some other works antisolvent crystallization was applied in the production of anhydrous crystals. For instance Oosterhof et al. (2001) studied production of anhydrous sodium carbonate at room temperature using ethylene glycol and diethylene glycol as antisolvents. Unlike conventional crystallization methods that cannot produce anhydrous sodium carbonate (due to its instability in aqueous solutions at temperatures lower than boiling point of saturated soda ash solution), their method incorporating antisolvent showed success in doing so.

Zhou et al. (2006) have carried out concentration controlled seeded antisolvent crystallization of a pharmaceutical compound using an algebraic equation for the solubility as a function of % solvent. The main objective of their feedback concentration control system was to keep the supersaturation low and constant. For this, different constant supersaturation values were investigated and their influence over nucleation discussed. In addition, they present simulation results investigating the antisolvent crystallization of paracetamol.

Nonoyama et al. (2006) also present a simulation study on seeded solvent crystallization of an active pharmaceutical ingredient (API) by water addition to original solution. The model they incorporate neglects nucleation, breakage and agglomeration, and only considers a size independent growth kinetic derived from experimental studies. Their investigation avoids nucleation of undesired polymorph by keeping supersaturation at a certain level.

In spite of all the previous works, there still exists a big gap in the control of the product crystal properties to desired values. Model-based dynamic optimization to determine optimal antisolvent crystallization strategies are poised to fill this gap and as far as the authors are aware, are not currently found in the literature.

In this work, a population balance model for antisolvent mediated crystallization is developed, implemented and validated against experimental data. Optimization-based parameter estimation is used to arrive at solubility and kinetic sub-models. Model-based dynamic optimization studies were performed using the identified model calculating repeatable the optimal antisolvent feed trajectories for a range of particle size objectives. These optimization studies were validated experimentally by implementation within a distributed control system (DCS) environment.

2. MODEL DEVELOPMENT AND IDENTIFICATION

Since the crystallization process is a particulate one, the population balance equation (PBE) as proposed by Hulburt and Katz (1964) is used accounting for the evolution of crystal particles across temporal and size domains. For a batch crystallization system with crystal growth assumed to be non-dispersed and independent of crystal size and where agglomeration and attrition are considered negligible, the PBE simplifies to

$$\frac{\partial n(L,t)}{\partial t} = -G\frac{\partial n(L,t)}{\partial L} + B \qquad (1)$$

where $n(L,t)$ is the number density of crystals, t is time, L is the characteristic crystal size, G is the growth rate of the crystals and B is the nucleation rate which is equal to zero for all sizes but the first. The model was solved in gPROMS environment (Process Systems Enterprise Ltd, UK) using backward finite discretization across the size domain, transforming the PBE into a set of differential equations. The solubility and kinetic sub-models are discussed in the next sections with respect to the NaCl-water-ethanol system which is used in this study as the model antisolvent crystallization system.

2.1 Solubility Model Identification

Knowledge of the equilibrium condition (solubility) of the crystallization system is crucial to the control of the particle size. We develop a model describing the solubility of the NaCl in the solvent-antisolvent mixture based on experimental solubility data (Yeo et al. 2006). This data corroborates with other data presented elsewhere for the same ternary system (Farelo et al., 2004). This model describing the

saturated concentration dependence on solvent concentration in solute free mixture is shown in Equation 2,

$$C^* = \frac{K(1-X)}{K+X} C^*_{water} \quad (2)$$

where C^* is the molality of solute in the mixture and C^*_{water} is molality of solute in pure water and has a value of 33.80 gram/100 grams of water of at constant temperature 25°C. K, like C^*_{water} is constant at constant temperature and is equal to 0.83094. X is the mass fraction of antisolvent in solute-free mixture.

2.2 Kinetic Model Identification

With respect to the modeling of antisolvent crystallization, limited work has been presented in the literature. No comprehensive studies are available that address model-based studies in this field. The best research addressing the antisolvent kinetics of nucleation and growth seems to be that of Jones and Mydlarz's (1990). In their study, they develop kinetic models for MSMPR crystallization. Their growth rate model is size dependent while its kinetic parameters are functions of antisolvent to water weight ratio. In another work, Mydlarz and Jones (1991) consider agglomeration kinetics in addition to nucleation and growth. Later, Nyvlt (1992) in his work mathematically investigates a kinetic model for nucleation rate. His model is a function of growth rate and supersaturation which depends on antisolvent addition rate. Nyvelt's conclusion suggests that the antisolvent addition should be slow in the early stages of the batch and increase proportionally with the crystal surface area. Such kinetic model developments are rare in the literature and present an opportunity to repostulate the mechanisms behind such complex kinetic phenomena.

In this study we incorporate a growth kinetic formulation proposed by Linnikov (2006) who neglected the effect of secondary nucleation and implemented seed addition. Seeding is not considered in the current study, and so a nucleation kinetic model is needed. Such a nucleation model is not available in the literature, however kinetics for cooling crystallization of sodium chloride as reported by Akal et al. (1986) are used. Together, the growth kinetics of Linnikov (2006) and nucleation kinetics of Akal et al. (1986) are referred to as 'Literature' kinetics in the rest of the paper. The Literature kinetic model is refined in this study via an optimization based (maximum likelihood criteria available from gEST function in gPROMS) parameter estimation. For this estimation step and model refinement, three experiments were conducted under antisolvent feeding conditions. The kinetic parameter set that provides the highest probability of the model predicting the real data from these three experiments was identified. The final nucleation and growth models settled at are

$$B = k_b \Delta C^b M_T \quad (3)$$

$$G = k_g \Delta C e^{-E/RT} \quad (4)$$

respectively, where ΔC is the supersaturation, k_b and b are the nucleation rate parameters, M_T is the magma density, k_g and E are growth rate parameters.

3. EXPERIMENTAL

Figure 1 shows the schematic of the experimental apparatus, instrumentation and control system. In all experiments, purified water by a Milli-Q system was used. The purities of sodium chloride (NaCl) salt (Merck) and ethanol (Merck) used in the experiments were 99.5% and 99.9% respectively.

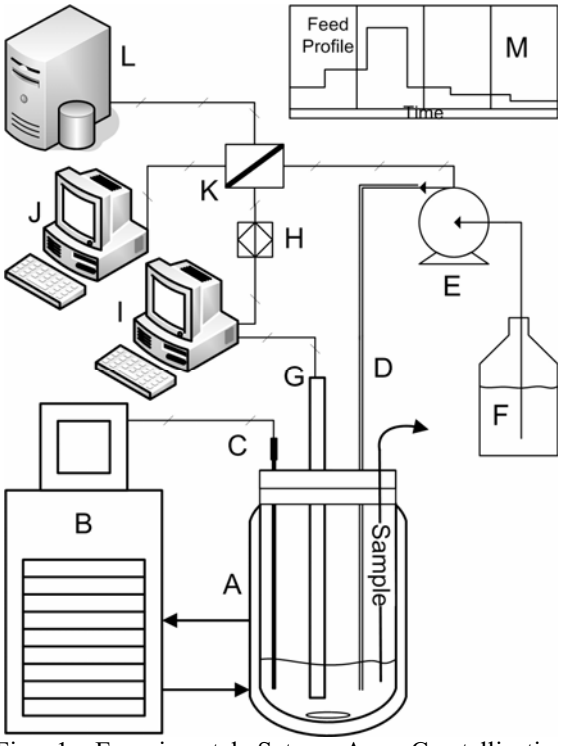

Fig. 1. Experimental Setup. A - Crystallization vessel, B - Temperature control system, C - Pt100 thermocouple, D - Ethanol addition line, E - Pump, F - Ethanol reservoir, G - FBRM probe, H - Analogue output card, I - FBRM control computer, J - DCS Station, K - Controller I/O terminals, L - DCS server, M - Feed profile to pump.

Ethanol was added to the aqueous NaCl solution using a calibrated digital dosing pump (Grundfos, Denmark). The ethanol addition profile was implemented and controlled from within a distributed control system (DCS) environment (Honeywell, USA). Temperature was controlled, at 25°C for all experiments, using a Pt100 thermocouple connected to heating/cooling circulator (Lauda, Germany). Particle chord length was measured online every 2 seconds using focused beam reflectance measurement (FBRM) probe (Mettler-Toledo

Lasentec Products, USA). Infrequent samples were removed iso-kinetically from the crystallizer and particle size was measured offline using Mastersizer 2000 particle size analyser (Malvern Instruments, UK). The FBRM signal was converted to 4-20 mA signals using an 8-channel analogue output PCI card inserted in the FBRM computer. This was then connected to the DCS for data monitoring and archiving.

4. MODEL-BASED OPTIMAL STRATEGY

The mathematical description of the proposed dynamic optimization problem (DOP) can be summarized as follows (Nowee et al., 2006):

$$
\begin{aligned}
&\underset{t,u(t),v,t\in[0,t_f]}{Min} \; z(t_f) \\
&F(x(t),\dot{x}(t),y(t),v)=0; t\in[0,t_f] \\
&l(\dot{x}(0),x(0),y(0),v)=0 \\
&t_f^{\min}\le t_f\le t_f^{\max} \\
&u^{\min}(t)\le u(t)\le u^{\max}(t), t\in[0,t_f] \\
&v^{\min}(t)\le v\le v^{\max} \\
&w_{el}^{\min}\le w(t_f)\le w_{el} \\
&w_{ee}(t_f)=w_{ee}^{tgt} \\
&w_{tt}^{\min}(t)\le w(t)\le w_{tt}(t), t\in[0,t_f] \\
&w^{\min}(t)\le w(t)\le w^{\max}(t), t\in[0,t_f]
\end{aligned}
\tag{5}
$$

Equation (5) indicates that the optimization (minimization) is performed considering the variable $z(t_f)$ as performance measure or objective function. Without any loss of generality, the objective function is simply the magnitude of a variable $z(t)$ evaluated at the end of the optimization horizon $t=t_f$. In addition, Equation (5) denotes the fact that the decision variables of the optimization problem are the time horizon t_f (a scalar) and a subset of variables given by the vectors u and v. The former denotes control variables that are allowed to vary according to the functionality $u(t)$ over the span of the time horizon $t\in[0,t_f]$. The latter indicates parametric variables that are fixed at a value v. F and l simply denotes the set of differential-algebraic equations (DAEs) encompassing the fundamental process model and the set of additional equations (initial conditions) that must be satisfied at the beginning of the optimization horizon (in these equations, x and y denote differential and algebraic variables respectively). In addition, we have lower and upper bounds on the decision variables, indicated by the superscripts min and max respectively. These constraints on the decision variables are stated explicitly since modern optimization algorithms can handle them very efficiently. This is not generally the case of other types of constraints. Then we have the end-point constraint variables, which usually represent certain conditions that the process system must satisfy at the end of the optimization horizon. For convenience, end-point constraints are divided into inequality and equality constraints. Although, the latter are a special case of the former, differentiating them simplifies the definition of some optimization problems. Also we include the interior-point constraint variables, which are used to enforce process variables to lie within the defined upper and lower bounds at any other time but the end of the optimization horizon. By definition, these are inequality constraints. Finally, we have the inequality path constraints. The reader should be aware that state-of-the-art declarative languages such as gPROMS do not support the high-level declaration of these constraints. For instance, Vassiliadis et al. (1994b) suggested to incorporate path constraints into the problem formulation by defining an appropriate auxiliary relationship denoting the magnitude of the constraint violation and adding an appropriate terminal condition in the form of an end-point constraint.

In this particular application, ten control intervals were implemented and the time horizon and system decision variables are subject to the following bounds:

Time horizon: $1800 \le t_f \le 16000$ s (6)
Initial concentration: $C_i \le 33.80$ gr/100gr water (7)
Ethanol federate: $0.375 \le F(t) \le 125$ml/min (8)

Subject to the following end-point constraints:

Final total volume: $100 \le V_{total} \le 500$ ml (9)
Final yield: $0 \le Y_{total} \le 20$ % (10)

Different size control related optimization objectives could be formulated as (1) keeping the supersaturation constant, (2) minimising nucleation, (3) maximising final mean size and (4) minimising the span of the size distribution. The results reported here correspond to maximization of final mean size for two cases, each with an additional end-point constraint specification in the final size range required:

Case 1: $100 \le \overline{L}(t_f) \le 500$ μm (11)

Case 2: $80 \le \overline{L}(t_f) \le 100$ μm (12)

5. RESULTS AND DISCUSSION

5.1 Kinetic Parameter Estimation

The parameter set $\theta = [k_b\ b\ k_g\ E]$ is determined from running three experiments under three antisolvent feeding profiles. The profile of the first of these experiments shown in Fig. 2 was determined via dynamic optimization based on the Literature kinetics. The data from this experiment were used to re-estimate (refine) the kinetic parameter set θ. The new value of θ was used in a subsequent dynamic optimization to determine a new optimal feeding profile (Figs. 3 & 4) which in turn was used in the other two experiments for further refining the value of θ. The results of the parameter estimation experiments are displayed in Figs 2-4 showing the

mean size profile of the refined kinetic model against the experimentally obtained mean size data. A satisfactory fit is obtained. The output from using the Literature kinetic model is also shown to show the level of refinement obtained. The final value of θ was estimated to be [7.339×10^5 1.76 824.7 4.902×10^4].

5.2 Dynamic optimal antisolvent feeding policy

Once the optimal kinetic model is attained, one can proceed to the subsequent step of model-based dynamic optimization. The idea that any final mean size could be obtained using the framework presented here was tested in two cases. In the first case, the objective function was to maximize the final mean size in an open range (Eq. 11). The dynamic optimization output is displayed in Fig. 5. The antisolvent feeding profile is shown to be slow initially and increased gradually in the middle of the batch. This corroborates with Nyvelt's (1992) results and is explained as follows. A slow addition rate leads to lower nucleation levels initially, until the accumulation of sufficient surface area for crystal growth to become dominant. To demonstrate the capability of this model-based optimal approach, we tested it using a different objective in Case 2 that of achieving a final mean particle size of specific range (Eq. 12). The optimal feed profile, unlike that in Case 1, resulted in much higher initial rate of addition (Fig. 6). In fact, it was more than 145 times greater in the optimization interval. The mean dynamic optimal mean size profiles for Cases 1 and 2 are presented in Figs. 7 and 8 respectively. We further validate these profiles experimentally and found very good agreements with the optimization (Figs 7 & 8). In Case 1 a final mean size of ~160 μm was achieved while in Case 2, the final mean size was at the upper bound of the specified (constrained) final size range.

The model-based approach presented here allows systematic and rapid process development of optimal operation of antisolvent crystallization generic to be readily implemented for control of particle size of pharmaceuticals or fine chemicals compounds.

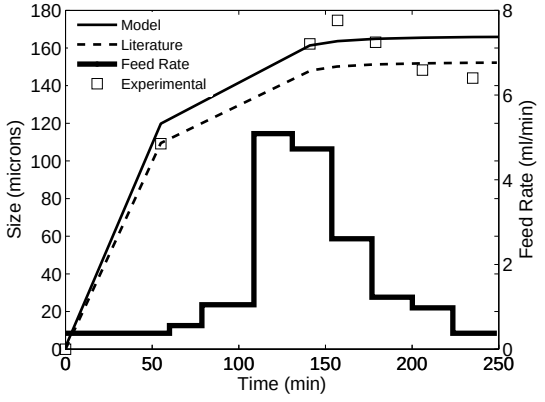

Fig. 2. Experiment 1 overlay plot of experimental mean size and model predictions using identified kinetics and those by Literature.

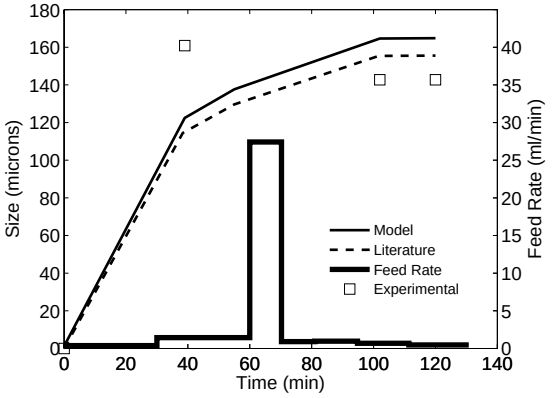

Fig. 3. Experiment 2 overlay plot of experimental mean size and model predictions using identified kinetics and those by Literature.

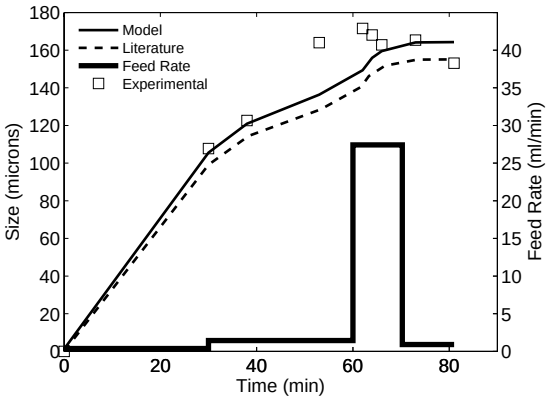

Fig. 4. Experiment 3 overlay plot of experimental mean size and model predictions using identified kinetics and those by Literature.

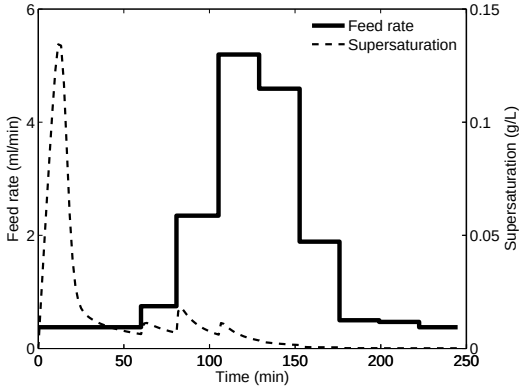

Fig. 5. Case 1 dynamic optimal strategy.

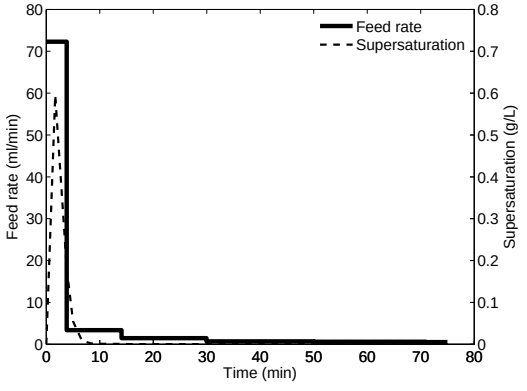

Fig. 6. Case 2 dynamic optimal strategy.

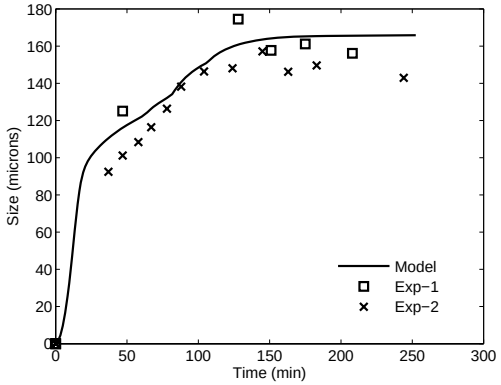

Fig. 7. Experimental validation of mean size results from optimal trajectory of Case 1.

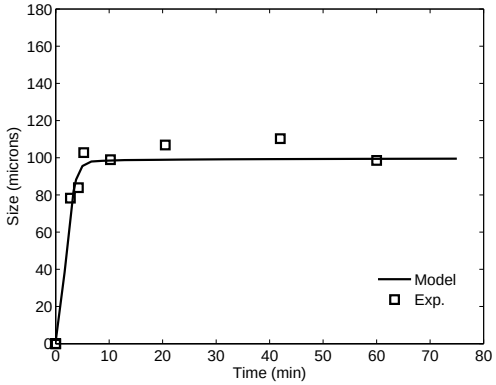

Fig. 8. Experimental validation of mean size results from optimal trajectory of Case 2.

REFERENCES

Akal, M. M., M. Zakaria, A. Ebrahim, M. M. Nassar (1986), Secondary nucleation rate of sodium chloride under different stirring conditions, *Journal of Crystal Growth*, **78,** 528-32.

Bakhbakhi, Y., P. Charpentier, and S. Rohani (2005), The solubility of phenanthrene in toluene: in situ ATR-FTIR, experimental measurement, and thermodynamic modeling. *Canadian Journal of Chemical Engineering*, **83,** 267-273.

Doki, N., N. Kubota, M. Yokota, S. Kimura, and S. Sasaki (2002), Production of sodium chloride crystals of uni-modal size distribution by batch dilution crystallization, *Journal of Chemical Engineering of Japan*, **35,** 1099-1104.

Farelo, F., A. M. C. Lopes, and M. I. Ferra (2004)., Solubilities of Sodium Chloride and Potassium Chloride in Water + Ethanol Mixtures from (298 to 323) K. *Journal of Chemical and Engineering Data*, **49,** 1782-1788.

Holmback, X. and A. C. Rasmuson (1999), Size and morphology of benzoic acid crystals produced by drowning-out crystallization, *Journal of Crystal Growth*, **198/199,** 780-788.

Hulburt, H. M. and S. Katz (1964), Problems in particle technology: A statistical mechanical formulation, *Chemical Engineering Science*, **19,** 555-74.

Kaneko, S., Y. Yamagami, H. Tochihara, and I. Hirasawa (2002), Effect of supersaturation on crystal size and number of crystals produced in antisolvent crystallization. *Journal of Chemical Engineering of Japan*, **35,** 1219-1223.

Kitamura, M. and M. Sugimoto (2003), Anti-solvent crystallization and transformation of thiazole-derivative polymorphs--I: effect of addition rate and initial concentrations. *Journal of Crystal Growth*, **257,** 177-184.

Linnikov, O. D. (2006). Spontaneous crystallization of sodium chloride from aqueous-ethanol solutions: Part 1 Kinetics and mechanism of the crystallization process, *Crystal Research and Technology*, **41,** 10-17.

Mydlarz, J. and A. G. Jones (1990), Potassium sulfate water-alcohols systems: composition and density of saturated solutions, *Journal of Chemical and Engineering Data*, **35,** 214-16.

Mydlarz, J. and A. G. Jones (1991), Crystallization and agglomeration kinetics during the batch drowning-out precipitation of potash alum with aqueous acetone, *Powder Technology*, **65,** 187-94.

Nonoyama, N., K. Hanaki, and Y. Yabuki (2006), Constant Supersaturation Control of Antisolvent-Addition Batch Crystallization, *Organic Process Research & Development*, **10,** 727-732.

Nowee, S. M., A. Abbas and J. A. Romagnoli (2006), Optimization in seeded cooling crystallization: a parameter estimation and dynamic optimization study, To appear in Chemical Engineering and Processing.

Nyvlt, J. (1992), Batch salting-out crystallization, *Chemical Engineering and Processing*, **31,** 39-42.

Oosterhof, H., G. J. Witkamp, and G. M. van Rosmalen (1999), Some antisolvents for crystallization of sodium carbonate, *Fluid Phase Equilibria*, **155,** 219-227.

Oosterhof, H., R. M. Geertman, G. J. Witkamp, and G. M. van Rosmalen (1999), The growth of sodium nitrate from mixtures of water and isopropoxyethanol, *Journal of Crystal Growth*, **198-199,** 754-759.

Rolandi, P. A. and J. A. Romagnoli (2003), Smart enterprise for pulp and paper: digester modeling and validation, *Computer-Aided Chemical Engineering*, **14,** 1049-1054.

Taboada, M. E., T. A. Graber, J. A. Asenjo, and B. A. Andrews (2000), Drowning-out crystallization of sodium sulphate using aqueous two-phase systems, *Journal of Chromatography, B: Biomedical Sciences and Applications*, **743,** 101-105.

Takiyama, H., T. Otsuhata, and M. Matsuoka (1998), Morphology of NaCl crystals in drowning-out precipitation operation, *Chemical Engineering Research and Design*, **76,** 809-814.

Vassiliadis, V.S., Sargent, R.W.H. and Pantelides, C.C. (1994b), Solution of a class of multistage dynamic optimization problems: 2 Problems with path constraints. *Industrial & Engineering Chemistry Research,* **33,** 2123-2133.

Yu, Z. Q., R. B. H. Tan, and P. S. Chow (2005), Effects of operating conditions on agglomeration and habit of paracetamol crystals in anti-solvent crystallization, Journal of Crystal Growth, **279**, 477-488.

Zhou, G. X., M. Fujiwara, X. Y. Woo, E. Rusli, H.-H. Tung, C. Starbuck, O. Davidson, Z. Ge, and R. D. Braatz (2006). Direct Design of Pharmaceutical Antisolvent Crystallization through Concentration Control. Crystal Growth & Design, **6**, 892-898.